UDK 519.61/.64:691:620.1
Original scientific article/Izvirni znanstveni članek

ISSN 1580-2949
MTAEC9, 47(5)621(2013)

APPLICATION OF INFINITE-ELEMENT CALCULATIONS FOR CONSOLIDATING A RAILWAY FOUNDATION OF BLOWING SAND RECLAMATION

UPORABA IZRAČUNA Z NESKONČNIMI ELEMENTI ZA UTRDITEV PODLAGE ŽELEZNIŠKE PROGE Z DROBNIM PESKOM

Kai-zhong Xie[1,2], Ying-zhong Pan[3], Hao Ni[1], Hong-wei Wang[1]

[1]Dept. Civil & Architecture Engineering of Guangxi University, Nanning, Guangxi, China
[2]Guangxi Key Laboratory of Disaster Prevention and Engineering Safety, Guangxi University, Guangxi, China
[3]Guangxi Railway Investment Group CO., LTD, Nanning, Guangxi, China
zhiwen54321@126.com

Prejem rokopisa – received: 2013-01-27; sprejem za objavo – accepted for publication: 2013-02-19

The dynamic-compaction method was adopted for consolidating a railway foundation of blowing sand reclamation in the North Bay of Guangxi, China. Based on the physical characteristics of the sands, the parameters of the infinite-finite elements for an extended Drucker-Prager model were obtained with the soil tests. This model was used to analyze the area of dynamic compaction and the mechanical behaviors of the sands under dynamic compactions with a dynamic explicit analysis. By comparing the test results, we demonstrated that dynamic compaction was an effective method for a railway foundation of blowing sand reclamation, and the numerical-analysis model based on the infinite-element method was a very powerful tool used in the actual conditions, having no boundary reflection under dynamic compactions.

Keywords: infinite element, dynamic compaction, blowing sand reclamation, explicit analysis, railway foundation

Za utrditev podlage železniške proge v North Bay, Guangxi, Kitajska, je bila uporabljena dinamična metoda kompaktiranja. Na podlagi fizikalnih lastnosti peskov in preizkusov tal so bili dobljeni parametri neskončno-končnih elementov za razširjeni Drucker-Pragerjev model. Tak model in dinamična eksplicitna analiza sta bila uporabljena za analizo področja dinamičnega kompaktiranja in mehanskih lastnosti peska pri dinamičnem kompaktiranju. S primerjavo rezultatov preizkusov smo pokazali, da je dinamično kompaktiranje peska učinkovita metoda za utrjevanje podlage železniške proge. Model za numerično analizo, ki temelji na metodi končnih elementov, je močno orodje brez omejitev v realnih razmerah dinamičnega kompaktiranja.

Ključne besede: neskončni element, dinamično kompaktiranje, droben pesek, eksplicitna analiza, podlaga železniške proge

1 INTRODUCTION

To construct highways and railways in the coastal region, in many sections blowing sand reclamation is used for constructing the foundation of the roads. The key problem of this kind of engineering is how to construct, economically and efficiently, large volumes of blowing-sand-reclamation foundations. There are many methods for consolidating a foundation of blowing sand reclamation, such as vibro-replacement stone pile, dynamic compaction, water-soil whip pile, and filler-vibration impact. For an estimation of the main construction parameters (the effective strengthening depth and radius) in the foundation treatment with the dynamic-compaction method, Li[1] built a three-dimensional finite-element model with LS-DYNA to get a numerical calculation of the single-point pounder strike of the kinetics process (a dynamic-compaction-method estimation based on a three-dimensional soil-dynamics numerical simulation). Li et al.[2] developed an estimation method and a formula for a dynamic-compaction foundation settlement in collapsible loess areas with a dynamic-compaction foundation-settlement-theory deduction, error analysis and measured-data verification. Mostafa[3] developed two-dimensional and three-dimensional finite-element models to study the dynamic compaction in cohesive soils.

In order to analyze the effect of the dynamic-compaction method, which is applied in the blowing-sand-reclamation projects in the coastal regions, we built an infinite-finite-element coupling model of the blowing-sand-reclamation foundation by introducing the infinite-element method providing the boundaries of the three-dimensional numerical model.

2 SPATIAL INFINITE-ELEMENT METHOD

Infinite elements are used for the boundary-value problems defined in unbounded domains or the problems, in which the region of interest is small in size, compared to the surrounding medium, and are usually used in conjunction with finite elements.

The static behavior of the infinite elements is based on modeling the basic solution variable u (in the stress analysis u is a displacement component) with respect to the spatial distance r measured from a "pole" of the solution, so that $u \to 0$ as $r \to \infty$, and $u \to \infty$ as $r \to 0$. The

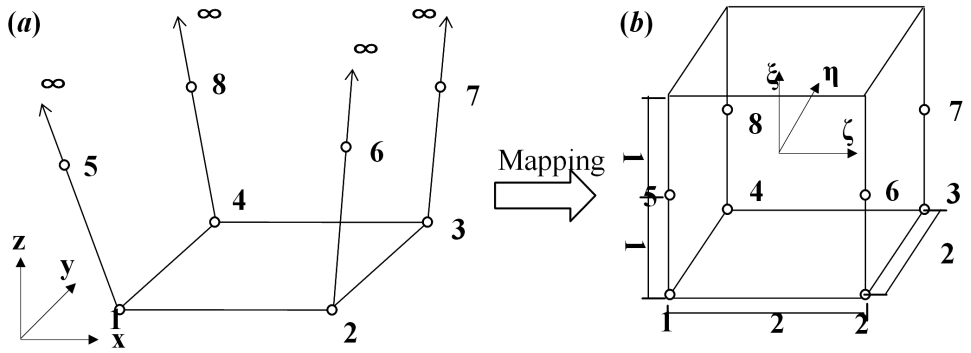

Figure 1: Node spatial mapping of an infinite element: a) practical element, b) parent element
Slika 1: Prostorska razporeditev vozlišč neskončnega elementa: a) praktični element, b) osnovni element

interpolation provides the terms of order $1/r$, $1/r^2$ and, when the solution variable is a stress-like variable (such as the pore liquid pressure in an analysis of the flow through a porous medium), also $1/r^3$. The far-field behavior in many common cases, such as a point load on a half-space, is thereby included. This modeling is achieved by using the standard cubic interpolation for $u(s)$ in $-1 \leq r \leq 1$, where s is a mapped coordinate that is chosen so that the mapping causes $r(s)$. We obtained a three-dimensional model of domains reaching infinity by combining this interpolation in the s-direction of a product form with the standard linear or quadratic interpolation in orthogonal directions in the mapped space.

Three-dimensional infinite elements only map the infinite domain along one direction, as shown on **Figure 1**, where the elements along the x and y directions are finite, while the z direction is infinite. After using a coordinate transformation, we can map the practical element of the xyz coordinates in a spatial cube element where the length of each side is 2.

The conversion relationship between the whole coordinates $x - y - z$ and the local coordinate is:

$$x = \sum_{i=1}^{n} M_i x_i \quad y = \sum_{i=1}^{n} M_i y_i \quad z = \sum_{i=1}^{n} M_i z_i \tag{1}$$

in which n is the node number, M_i is the mapping function, and x_i, y_i, z_i are the nodal coordinates:

$$M_1 = \frac{(1-\xi)(1-\eta)(-\zeta)}{2(1-\zeta)} \qquad M_2 = \frac{(1+\xi)(1-\eta)(-\zeta)}{2(1-\zeta)}$$

$$M_3 = \frac{(1+\xi)(1+\eta)(-\zeta)}{2(1-\zeta)} \qquad M_4 = \frac{(1-\xi)(1+\eta)(-\zeta)}{2(1-\zeta)}$$

$$M_5 = \frac{(1-\xi)(1-\eta)(1+\zeta)}{4(1-\zeta)} \qquad M_6 = \frac{(1+\xi)(1-\eta)(1+\zeta)}{4(1-\zeta)}$$

$$M_7 = \frac{(1+\xi)(1+\eta)(1+\zeta)}{4(1-\zeta)} \qquad M_8 = \frac{(1-\xi)(1+\eta)(1+\zeta)}{4(1-\zeta)} \tag{2}$$

When practical elements are mapped to be parent elements, we can analyze the characteristics of the parent elements. If we assume that the parent elements use the same shape function as the 8-node spatial elements, they can couple with the 8-node spatial finite elements. The selection of a displacement model is as follows:

$$u = \sum_{i=0}^{n} N_i u_i \quad v = \sum_{i=0}^{n} N_i v_i \quad w = \sum_{i=0}^{n} N_i w_i \tag{3}$$

where n is the node number, N_i is the mapping function and u_i, v_i, w_i are the nodal displacements:

$$\begin{aligned}
N_1 &= 0.125(1-\xi)(1-\eta)(\zeta^2-\zeta)\\
N_2 &= 0.125(1+\xi)(1-\eta)(\zeta^2-\zeta)\\
N_3 &= 0.125(1+\xi)(1+\eta)(\zeta^2-\zeta)\\
N_4 &= 0.125(1-\xi)(1+\eta)(\zeta^2-\zeta)\\
N_5 &= 0.25(1-\xi)(1-\eta)(1-\zeta^2)\\
N_6 &= 0.25(1+\xi)(1-\eta)(1-\zeta^2)\\
N_7 &= 0.25(1+\xi)(1-\eta)(1-\zeta^2)\\
N_8 &= 0.25(1-\xi)(1+\eta)(1-\zeta^2)
\end{aligned} \tag{4}$$

3 CONSTITUTIVE MODEL OF THE SAND SOILS

For a non-metal particle material such as soil and rock, we can adopt a D-P model that can simulate a non-metal material, extending its function on the basis of an ideal elastic-plastic model.

The Drucker-Prager ideal elastic-plastic model is one of the earliest constitutive models for elastic-plastic geotechnical materials; its parameters are few and the calculation is simple.[4,5] Its yield-criterion expression is shown in equation (5):

$$F(\sigma_{ij}) = \sqrt{J_2} - \alpha I_1 - K = 0 \tag{5}$$

where J_2 is the second invariant of the stress-deviation tensors, I_1 is the first invariant of the stress deviation tensors and α, K are the material constants. As Drucker and Prager derived the relations between α, K and the material constants C, φ of the Mohr-Coulomb criterion is shown in equation (6):

$$K = \frac{\sqrt{3}\cos\varphi}{\sqrt{3+\sin^2\varphi}} \quad \alpha = \frac{\sin\varphi}{\sqrt{3}\sqrt{3+\sin^2\varphi}} \tag{6}$$

Drucker and Prager (1952) proposed a yield condition, according to which the yield surface is a cone in the

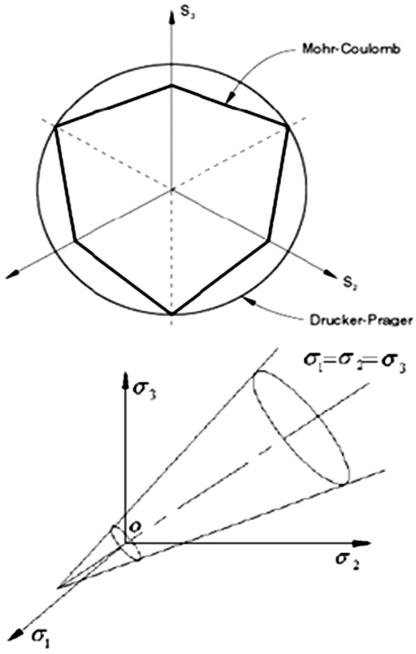

Figure 2: Generalized von Mises yield surface
Slika 2: Posplošena površina meje plastičnosti po von Misesu

stress space, as seen on **Figure 2**, on the π-plane, while its yield curve is a circle that is inscribed in the Mohr-Coulomb yield curve; in the stress space, its yield surface is a cone, while the center axis and the isocline are coincident.

The D-P model considers that when the material is in its elastic phase ($F < 0$) or unloading phase ($F = 0$, and $\delta F < 0$), the stress-strain relation shown in equation (7) applies:

$$\sigma_{ij} = K\sigma\varepsilon_{KK}\delta_{ij} + 2G\delta\varepsilon_{ij} \tag{7}$$

If $F = 0$ and the loading is ($\delta F > 0$), the stress-strain relation shown in equation (8) applies:

$$\delta\sigma_{ij} = K\sigma\varepsilon_{KK}\delta_{ij} + 2G\delta\varepsilon_{ij} - d\lambda(-3K\alpha)\delta_{ij} + \frac{G\sigma_{ij}}{\sqrt{J_2}} \tag{8}$$

where $d\lambda = \dfrac{-3K\alpha\delta\varepsilon_{KK} + \dfrac{G}{\sqrt{J_2}}\sigma_{mn}\varepsilon_{mn}}{9K\alpha^2 + G}$;

δ_{ij} is the Kronecher sign; when $i = j$, $\delta_{ij} = 1$; when $i \neq j$, $\delta_{ij} = 0$; σ_{ij} indicates the stress tensors, ε_{ij} indicates the strain tensors; K is the volume-elastic modulus; G is the sheer-elastic modulus.

4 LINEAR DRUCKER-PRAGER MODEL

The linear model is written in terms of all three stress invariants. It provides for a possible noncircular yield surface in the deviatoric plane matching different yield values of the triaxial tension and compression, the associated inelastic flow in the deviatoric plane, the separate dilation and friction angles.

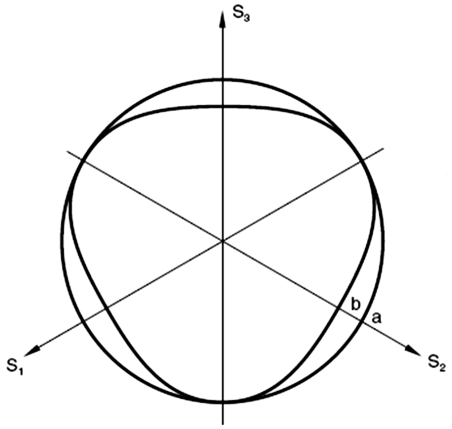

Figure 3: Typical yield/flow surfaces
Slika 3: Značilna mejna površina plastičnosti

(1) Yield criterion

The linear Drucker-Prager criterion is written as:

$$F = t - p\tan\beta - d = 0 \tag{9}$$

where:
$$t = \frac{1}{2}\theta\left[1 + \frac{1}{K} - \left(1 - \frac{1}{K}\right)\left(\frac{r}{\theta}\right)^3\right] \tag{10}$$

$\beta(\theta,f_i)$ is the slope of the linear yield surface in the $p - t$ stress plane and is commonly referred to as the friction angle of the material; d is the cohesion of the material; $K(\theta,f_i)$ is the ratio of the yield stress in the triaxial tension to the yield stress in the triaxial compression, thus, controlling the dependence of the yield surface on the value of the intermediate principal stress (as seen in **Figure 3**). θ is the temperature, $f_i(i = 1, 2, ...)$ refers to the other predefined field variables.

The cohesion d of the material is related to the input data as:

$$d = \left(1 - \frac{1}{3}\tan\beta\right) \qquad \sigma_c = \left(\frac{1}{K} + \frac{1}{3}\tan\beta\right)$$
$$\sigma_t = \frac{\sqrt{3}}{2}\tau\left(1 + \frac{1}{K}\right) \tag{11}$$

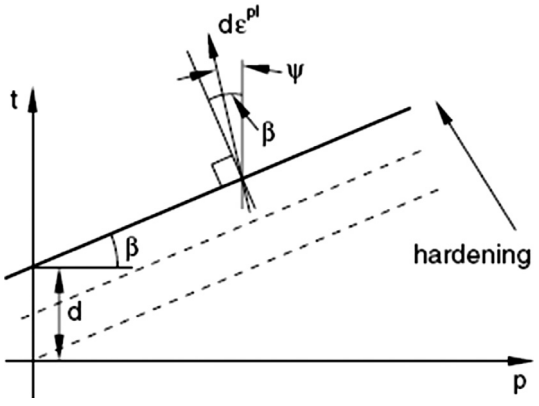

Figure 4: Yield surface and flow direction
Slika 4: Meja plastičnosti in smer toka materiala

where σ_c is the uniaxial compression yield stress, σ_t is the uniaxial tension yield stress and τ is the shear stress.

(2) Plastic flow

G is the flow potential, chosen in this model as:

$$G = t - p\tan\psi_1 \tag{12}$$

where $\psi_1(\theta, f_i)$ is the dilation angle in the $p - t$ plane. A geometric interpretation of ψ is shown in the $p - t$ diagram of **Figure 4**. In the case of the hardening defined for the uniaxial compression, this flow-rule definition precludes the dilation angles tan $\psi > 3$. This restriction is not seen as a limitation since it is unlikely that it will apply to real materials.

(4) Non-associated flow

The non-associated flow implies that the material stiffness matrix is not symmetric; therefore, the unsymmetrical matrix storage and solution scheme should be used. If the difference between β and ψ is not large and the region of the model, in which the inelastic deformation is occurring is confined, it is possible that a symmetric approximation of the material stiffness matrix will give an acceptable rate of convergence and the unsymmetrical matrix scheme may not be needed.

5 LOADING FORM OF DYNAMIC COMPACTION

According to the previous research and test demonstrations, in the process of a pounder's collision with and impact on a foundation, the contact stress has only one significant peak value on the time-history curve and its duration is very short, around 0.1 s. The impact load is simplified into the load of the triangle form, as seen on **Figure 5**. The values of t_n, t_r, P_{max} from this figure can be measured in the test fields or estimated with the following formulas:

$$P_{\max} = \frac{V_0\sqrt{mS}}{\pi r^2} \quad t_n = \pi\sqrt{\frac{m}{S}} \quad t_r = \left(\frac{1}{4} \approx \frac{1}{2}\right)t_n \tag{13}$$

where V_0 is the landing speed of the pounder, m is the pounder quality, r is the pounder radius and S is the elastic constant:

$$S = 2rE(1-\mu^2) \tag{14}$$

As the deformation modulus of the soil is being continuously adjusted, the contact stress and the contact time also undergo continuous changes. We fully considered these changes in the simulation, adjusting, on the basis of the deformation modulus, the contact stress and the contact time for each analysis step, where one pounder strike is defined as one analysis step, lasting for 0.3 s, so that the total analysis time is 2.1 s.

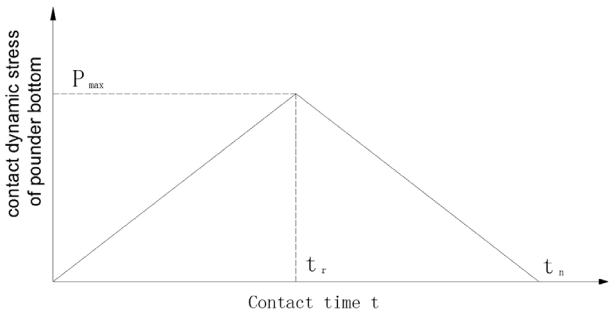

Figure 5: Strong-pounder dynamic-effect model
Slika 5: Model dinamičnega učinka močnega tolkača

6 PROJECT APPLICATION

A section of the railway branch between DaLanPing and BaoShuiGang (CK12+ 000 ~ CK17+300) is involved in a blowing-sand-reclamation project applying to a littoral area with the total length of the dynamic compaction area set to be 150 m.

The section from DK15+315.64 to DK15+515.64 was regarded as the test section. According to the depth range covered with the standard penetration test, the area was geotechnically divided into 3 layers: the filling sand, the fine sand and the mud.

7 NUMERICAL ANALYSIS

7.1 Analysis model

With the ABAQUS finite-element software, simulating the foundation of blowing sand reclamation and using a dynamic-compaction method, we built two three-dimensional entity models on the basis of the finite-element model and infinite-finite element coupling model, aiming to simulate the dynamic compaction process for the test section.

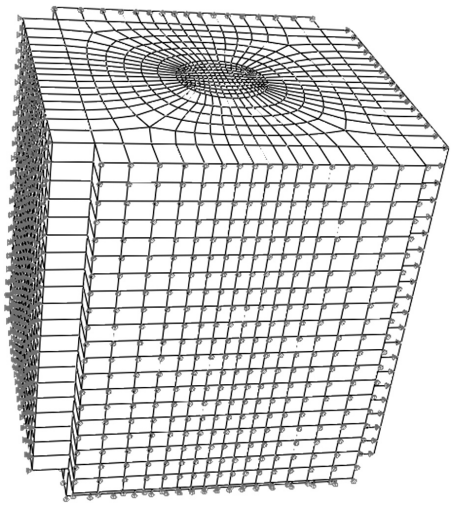

Figure 6: Finite-element method
Slika 6: Metoda končnega elementa

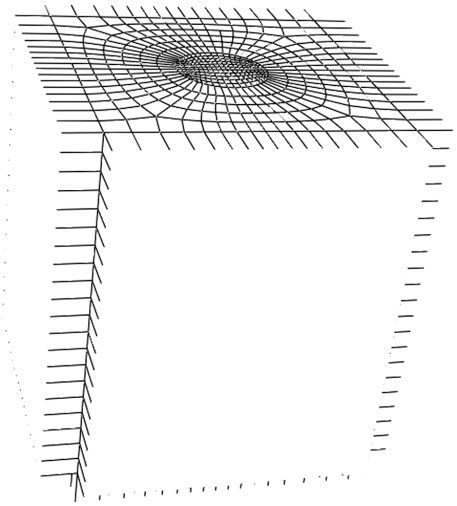

Figure 7: Coupling method of an infinite-finite element
Slika 7: Združena metoda neskončnega-končnega elementa

The factors influencing the foundation of blowing sand reclamation, included in the dynamic-compaction method, are many and the deformation characteristics of the soil body are also very complicated, so we introduced the following assumptions:

1) The soil body in the model can be regarded as homogeneous, isotropic and elastic-plastic infinite spatial.
2) No effects of the groundwater need to be considered.
3) The pounder is simplified into a force, that is, a force is applied on the soil body.
4) The interface between the above force and the tangential force of the blowing sand reclamation can be ignored.

The finite-element model (model 1) is based on the following parameters: the width of the top surface of the roadbed is 20 m, the width of the bottom surface is 40 m, the height is 10 m, the length is 10 m, and the grid size is 1 m. The tamper weight is 150 kN, the tamping energy is 2600 kN m.

The infinite-finite-element coupling model (model 2) is based on the finite-element model. The boundary elements for four weeks and the bottom elements can be replaced with the spatial infinite elements. As the infinite elements belong to the boundary elements, we do not need to set the boundary conditions, as shown in **Figures 6** and **7**.

7.2 Material model parameters

The physical and mechanical parameters of different sections between the top and the bottom of the filling-sand layer are presented in **Table 1**.

Table 1: Physical and mechanical parameters of the filling-sand layer
Tabela 1: Fizikalni in mehanski parametri plasti polnilnega peska

Sand layer	E/MPa	μ	β/°	K	ψ/°	ε_p	σ/kPa
0≈1 m	8	0.3	58.5	0.778	0	0	100
1≈2 m	14.5	0.3	58.5	0.778	0	0	140
2≈5 m	19	0.3	58.5	0.778	0	0	180
5≈6 m	8	0.3	58.5	0.778	0	0	100
6≈8 m	14.5	0.3	58.5	0.778	0	0	140
8–12 m	18	0.3	58.5	0.778	0	0	180

Table 2: Settlement of dynamic compaction (cm)
Tabela 2: Posedanje pri dinamičnem kompaktiranju (cm)

times	test	model 1	model 2
1	35.7	36.0	40.0
2	19.0	21.0	25.0
3	16.7	12.0	14.0
4	12.3	10.0	12.0
5	8.7	5.0	7.0
6	6.0	3.0	5.5
7	3.0	1.0	2.0
total	101.4	88.0	105.5

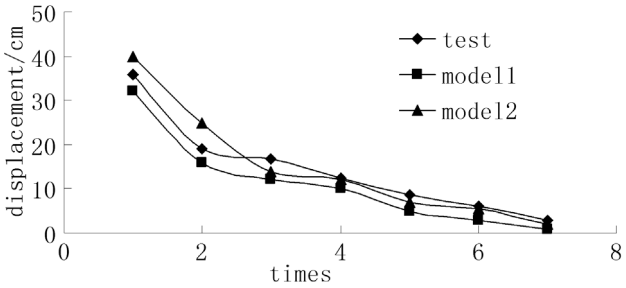

Figure 8: Relation curve of dynamic pit settlement and times
Slika 8: Odvisnost krivulje dinamičnega posedanja od ponovitev

We simulated and analyzed the dynamic compaction process for different test sections with two models, and compared the analysis results with the measured values of the field dynamic-penetration test. The surface-settlement data of dynamic compaction for the process of 7 strikes is presented in **Table 2** and the dynamic-compaction settlements are plotted in **Figure 8**.

As shown in the above figure and table, in the numerical analysis of consolidating the foundation's capacity for blowing sand reclamation, the settlement amount for model 1 using the finite-element method is smaller than for model 2 using the infinite-finite element method with the infinite element as the boundary condition. The values of model 2 are close to the measured values of the field test, showing that this model can simulate the practical boundary conditions well by introducing infinite elements to the analysis model.

In the process of dynamic compaction, when the number of the rammer strikes is 7, the settlement tends to be stable and the measured value is 3 cm, reaching the settlement requirement of dynamic compaction.

8 CONCLUSIONS

On the basis of an analysis of the foundation's capacity for blowing sand reclamation carried out with the

dynamic-compaction method, and a comparison of its results with the measured values, we can draw the following conclusions:

1) The model can simulate the practical conditions well by introducing the infinite elements as boundaries;
2) The boundary conditions have a big influence on the calculation results of the finite-element method;
3) Compared with the measured values, the values of model 2 that used the infinite element as the boundary condition are close to the measured values;
4) If the number of the rammer strike is 7, the settlement tends to be stable, reaching the requirement of dynamic compaction.

Acknowledgements

Xie thanks the National Natural Science Foundation of China (No.: 51068001), the Systematic Project of the Guangxi Key Laboratory of Disaster Prevention and Structural Safety – the Scientific Research (2012ZDX04), the Technology Development Key Project of Guangxi (No.: 0816006-7 and No.: 0992027-12) and the Scientific Research Foundation of the Guangxi University (No.: XBZ100762).

9 REFERENCES

[1] J. Li, W. F. Teng, Estimation of construction parameters of dynamic compaction method based on 3D soil dynamic numerical simulation, Yangtze River, 42 (**2011**) 15, 50–52

[2] W. Li, Q. Gu, L. Su, B. Yang, Finite element analysis of dynamic compaction in soft foundation, Procedia Engineering, 12 (**2011**), 224–228

[3] K. Mostafa, Numerical modeling of dynamic compaction in cohesive soils, A Dissertation Presented to The Graduate Faculty of The University of Akron, 2010, 2–3

[4] J. P. Borg, J. R. Cogar, A. Lloyd, A. Ward, D. Chapman, K. Tsembelis, Computational simulations of the dynamic compaction of porous media, International Journal of Impact Engineering, 33 (**2006**), 109–118

[5] L. Chen, Application and Research of Ground Treatment of Encircling the Sea to Land Project, Special Structure, 27 (**2010**) 2, 1–5